# The Impact of Phenological Variation on Texture Measures of Remotely Sensed Imagery

Patrick D. Culbert, Anna M. Pidgeon, Véronique St.-Louis, Dallas Bash, and Volker C. Radeloff

***Abstract*—Measures of image texture derived from remotely sensed imagery have proven useful in many applications. However, when using multitemporal imagery or multiple images to cover a large study area, it is important to understand how image texture measures are affected by surface phenology. Our goal was to characterize the robustness to phenological variation of common first- and second-order texture measures of satellite imagery. Three North American study sites were chosen to represent different biomes. At each site, a suite of image textures were calculated for three to four dates across the growing season. Texture measures were compared among dates to quantify their stability, and the stability of measures was also compared between biomes. Interseasonal variability of texture measures was high overall $(\mathrm{mean\ interseasonal\ coefficient\ of\ variation} = 0.79)$, indicating that care must be taken when using measures of texture at different phenological stages. Certain texture measures, such as first-order mean and entropy, as well as second-order homogeneity, entropy, and dissimilarity, were more robust to phenological change than other measures.**

***Index Terms*—Image texture analysis, remote sensing, vegetation.**

## I. Introduction

REMOTELY sensed images are composed of both tone (spectral variation) and texture (spatial variation) [1], [2]. While spectral information is relatively easy to quantify, texture is more difficult to quantify because it involves measurements of pattern variability, shape, and size [3]. Because of the difficulties in measurement and interpretation, texture has been less utilized in remote sensing than spectral analysis. This is unfortunate, because pixel-wise spectral analyses ignore the large amount of information present in image texture. The use of texture measures has been recognized as an important method for quantifying spatial heterogeneity, and its use has recently increased in studies of land cover classification [3]–[5], habitat modeling [6]–[8], and measurement of vegetation structure [8]–[10].

The most commonly used measures of texture are divided into two groups: first-order (occurrence) and second-order (co-occurrence) [11]. First-order measures are statistics calculated from the spectral values of pixels in a defined neighborhood, typically implemented as a moving window. Common first-order measures include minimum, maximum, range, mean, standard deviation, skewness, and kurtosis. Of these measures, standard deviation (or variance) is the most commonly used [3], [6], [7], [12]. First-order measures are limited in power because they quantify variation in spectral information without regard to the spatial arrangement within the moving window. However, first-order measures are computationally simple and can be quickly calculated over large spatial extents.

Second-order texture measures take into account the spatial distribution of spectral values [3]. These measures are derived from the gray-level co-occurrence matrix (GLCM) [11]. The GLCM is a symmetric n-by-n matrix, where n is the number of possible gray-tone values. Entries $\mathrm{P_{ij}}$ in the matrix, represent the relative frequency of pixels with tone levels $i$ and $j$ co-occurring at a user specified distance and direction [11]. There are four commonly used directions, 0° (horizontal), 45° (right diagonal), 90° (vertical), and 135° (left diagonal). The distance parameter, $d$, is typically set to 1, thus comparing adjacent pixels [13]. In multispectral imagery, a separate GLCM is computed for each band of interest.

The GLCM assumes that the texture information of an image can be represented in adjacency relationships between specific gray tones [14]. Similar to first-order measures, the GLCM is calculated for a neighborhood, typically a moving window. Haralick [11] originally proposed 14 texture measures derived from the GLCM: angular second moment, contrast, correlation, difference entropy, difference variance, entropy, information measures of correlation (two different features), inverse difference moment (now more commonly referred to as homogeneity), maximal correlation coefficient, sum average, sum entropy, sum of squares variance, and sum variance. Many of these original second-order measures have been found to be highly correlated, and a subset of six measures is considered most useful for remote sensing analysis: angular second moment (ASM), contrast, correlation, homogeneity, variance, and entropy, with the first three being the least correlated [2], [10].

Several types of remote sensing data analyses benefit from the inclusion of textural measures. Texture measures are frequently included as additional (or sole) inputs in image classifications. The use of texture measures is especially helpful in classifications of areas such as forests, where species may have similar spectral characteristics but different spatial patterns [3]–[5]. Measures of texture are also well-suited to quantify vegetation structure [15], including forest structure [10], forest age class [16], woody plant encroachment [17], and leaf area index [18]. More recently, habitat modeling studies have incorporated texture measures. For animals such as birds, vegetation structure is

Manuscript received November 07, 2008; revised March 23, 2009. First published May 19, 2009; current version published January 20, 2010. This work was supported in part by the National Aeronautics and Space Administration Biodiversity Program under Grant NNG06GJ00G and in part by the Strategic Environmental Research and Development Program.

P. D. Culbert, A. M. Pidgeon, V. St.-Louis, and V. C. Radeloff are with the Department of Forest and Wildlife Ecology, University of Wisconsin-Madison, Madison, WI 53706 USA (e-mail: pdculbert@wisc.edu).

D. Bash is with the Directorate of Environment, Fort Bliss, TX 79916 USA.

Color versions of one or more of the figures in this paper are available online at http://ieeexplore.ieee.org.

Digital Object Identifier 10.1109/JSTARS.2009.2021959

an important cue for habitat selection [19], [20]. Texture measures derived from remotely sensed imagery have proven useful in bird species presence/absence models [6], relating vegetation structure to habitat preference [7], [21], and modeling avian species richness [22], [23].

However, while the utilization of texture measures in remote sensing analyses is increasing, there is a significant issue that has thus far been mostly overlooked. Any texture analysis involving images of different areas or multitemporal images of the same area must take into account factors that may severely affect texture measures. Absolute texture comparisons between images are confounded by factors such as light angle, atmospheric effects [17], and vegetation phenology [24]. In particular, the effect of phenology could significantly affect multitemporal analyses. Even though these factors can introduce substantial problems to analyses, thus far, only a few studies have mentioned the possible effects of phenology on texture measures [24], [25], and none of these studies explicitly examined the effect.

At the same time, the potential upside of phenological variation in image texture is that texture differences among multitemporal images could contain important information. The analysis of temporal variation in image texture could thus yield insight into phenological processes and help distinguish different vegetation types. Texture measures derived from certain phenological stages will likely be better suited to specific purposes, such as plant species identification, and specific texture signatures related to a process or feature of interest may be more pronounced at specific phenological stages. To exploit these relationships, more understanding is needed on the behavior of specific texture measures in different biomes over the growing season and which parts of the growing season yield the best texture measures to be related to specific processes.

As computing power increases, so does the ability to carry out analyses over large spatial extents. The historical archive of remotely sensed imagery is growing, and data are becoming more freely available (as with the free release of the USGS Landsat archive). All of these factors will contribute to increases in multitemporal and large-spatial-extent analyses that utilize texture measures. Thus, both positive and negative implications of the effects of phenology on measures of image texture need more study.

The primary goal of our research was to determine how first- and second-order texture measures respond to changes in phenology. We were interested in finding the degree to which measures of image texture are robust to phenological change. In addition, we were interested in understanding how phenology-related variability in texture measures differs across different biomes, window sizes, and spectral bands.

We expected that image texture measures that are invariant to linear transformations of the digital numbers (e.g., angular second moment and entropy [11]) would be the most robust to phenological change. We also expected that measures of texture would vary the most in biomes with high seasonal variation in vegetation. Strong fine-scale variation in vegetation would lead to high spectral variation, which we expected would translate into higher variation of texture measures.

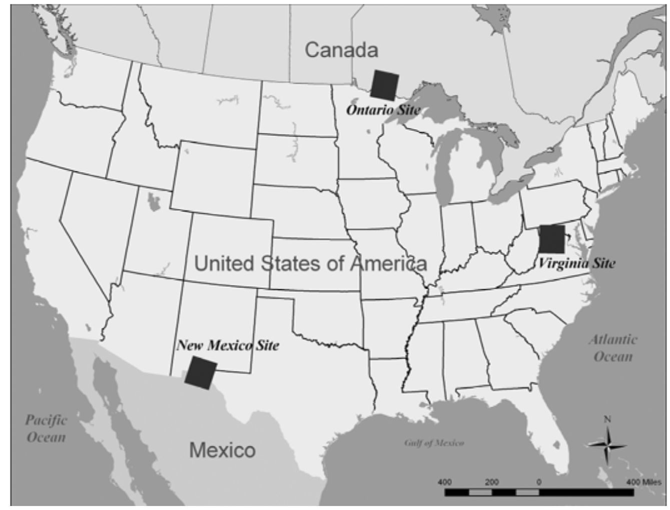


Fig. 1. Three study sites: Landsat path 16 row 33, along the border of New Mexico and Chihuahua, Mexico; path 33 row 38 along the border of Ontario, Canada, and Minnesota; and path 27 row 26, including parts of Virginia, West Virgina, and Maryland.

Texture measures are influenced by window size since the scale of the spatial patterns measured is dependant on window size, but we did not expect different window sizes to substantially differ in their response to phenological change. However, since a larger window contains a larger sample size, we predicted a slight reduction in variance. Lastly, we expected that variance of texture measures would not be uniform across spectral bands. In particular, we believed that Landsat TM band 4 would have higher interseasonal variability in texture measures because near-infrared reflectance is strongly correlated with vegetative vigor [26], which varies substantially across growing seasons.

## II. Methods

We calculated a suite of texture measures for three study sites representing different biomes, and for images acquired at different points in the growing season. The resulting texture measures were compared among image dates to determine which measures were most robust to change in surface phenology and whether ranking in terms of robustness was consistent among different biomes. We used several window sizes and spectral bands in order to analyze their effect on texture measure robustness to phenological variation.

Three study sites were chosen, representing contrasting biomes: a desert scrub region in New Mexico, a mix of deciduous and evergreen forests in Ontario, Canada, and an area of deciduous forest and agriculture in Virginia. These sites correspond to Landsat TM path 33 row 38, path 27 row 26, and path 16 row 33, respectively (Fig. 1).

The New Mexico site was centered near Las Cruces, NM, and includes areas of New Mexico, Texas, and Chihuahua, Mexico. The area was primarily desert scrubland of the Chihuahuan Desert Province [27], with relatively flat basins as well as mountainous areas. The Rio Grande River was a prominent feature in the scene, with a swath of agriculture approximately 5-mi wide running along the river. The metropolitan area of

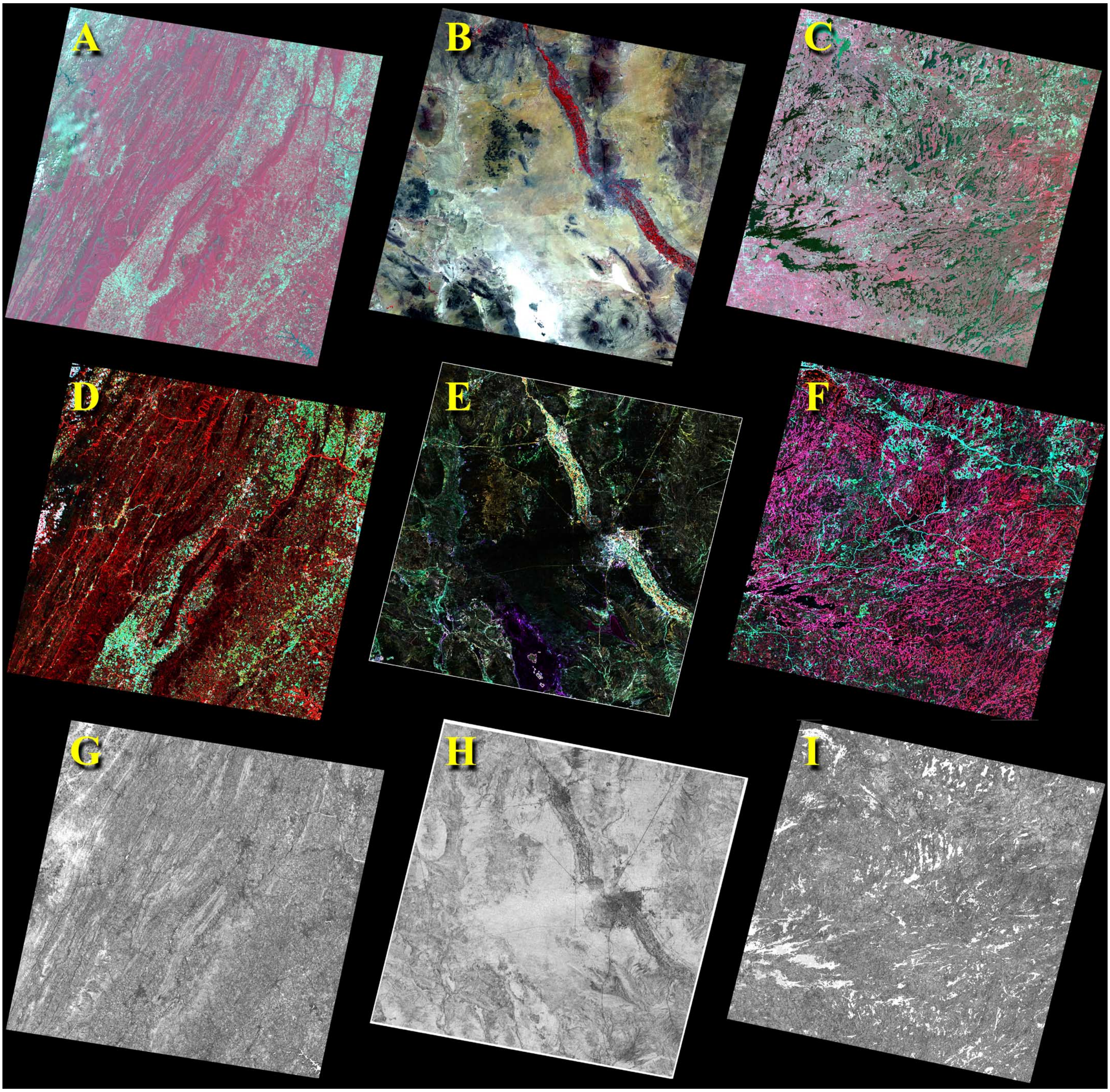


Fig. 2. (a)–(c) Virginia, New Mexico, and Ontario study sites, respectively, bands 4/3/2 false-color composite. (d)–(e) Second-order 11 × 11 variance of Virgina, New Mexico, and Ontario study sites, respectively, bands 4/3/2 false color composite. (g)–(i) Second-order 11 × 11 homogeneity of band 4 (near-infrared) of Virginia, New Mexico, and Virginia study sites, respectively.

El Paso, TX, and Ciudad Juárez, Mexico (population approximately 2.2 million) was included in the scene.

The Ontario study site covered mostly southwestern Ontario with a small area of northern Minnesota also included. The scene was in the Boreal Shield ecozone [28]. This area had a very low human population and was composed almost entirely of forests and small lakes. The forests were primarily evergreen or mixed evergreen/deciduous. Heavy forest harvesting was apparent in parts of the imagery.

The Virginia site included portions of western Maryland, eastern West Virginia, and Virginia. The West Virginia portion of the image was dominated by deciduous forests on slopes of the Appalachian Mountains, with some agriculture in the valleys. Agriculture dominated most of the Virginia portion of the image, with some mountainous deciduous forest, including nearly all of Shenandoah National Park. The area was primarily in the Central Appalachian Broadleaf Forest-Coniferous Forest-Meadow Province with a small section of Southeastern Mixed Forest Province [27].

For each study site, a collection of Landsat images was assembled with the goal of having mostly cloud free images spanning the growing season within a 1–3 year period

TABLE I
STUDY IMAGERY

| Site | Image Date (Sensor) |
|---|---|
| New Mexico | 04/23/2000 (ETM+)<br>06/13/2001 (ETM+)<br>09/12/1999 (ETM+) |
| Ontario | 04/29/2000 (ETM+)<br>05/21/2002 (ETM+)<br>07/05/2001 (ETM+)<br>09/12/2000 (TM) |
| Virginia | 03/31/2000 (ETM+)<br>10/15/1999 (TM)<br>05/24/2002 (ETM+) |

[Table I, Fig. 2(a)–(c)]. For the Ontario study site, approximately 15% of the 09/12/2000 image was affected by clouds and about 25% of the 04/29/2000 image was contaminated by smoke. In the Virginia site, the 05/24/2002 image contained 10% cloud cover. These affected areas were masked out from all images for the final analysis of each study site.

Within each study site, one image was chosen as the reference and the others were georeferenced to that image using Erdas Imagine Autosync [29]. A second order polynomial model was applied, and images were resampled using nearest neighbor interpolation. Images were projected in UTM NAD83 zones 13, 15, and 17 North for the New Mexico, Ontario, and Virginia study sites, respectively.

A suite of texture measures were calculated for each of the 10 images using ENVI [30] [Fig. 2(d)–(i), for example]. For each image band, first-order texture measures: mean, variance, entropy, and skewness were calculated using window sizes of $3 \times 3$, $7 \times 7$, and $11 \times 11$. The second-order texture measures: correlation, contrast, angular second moment, homogeneity, dissimilarity, entropy, and variance were also calculated for each band. When calculating second order measures, care must be taken to avoid sparsely populated GLCMs [11], [24]. With small window sizes, the number of pixel adjacencies is relatively small, and a GLCM of 8-bit data will have 65 536 cells ($256 \times 256$). This results in a value of 0 in most cells of the GLCM, causing instability in the texture measurement. For this reason, we calculated second-order measures with larger window sizes of $11 \times 11$ and $15 \times 15$, and we reduced the radiometric resolution to 6 bits (64 values, yielding a GLCM with 4 096 cells) instead of the 8 bits of the original data. GLCMs were calculated for the horizontal direction with a distance parameter of 1 pixel.

Within each study site, the calculated texture measures were compared among image dates on a pixel-by-pixel basis. Because variation in texture measures was consistently higher in pixels with a high mean texture value, the per-pixel coefficient of variation was chosen as a more representative measure of interseasonal variability. For each study site, band, texture measure, and window size combination, the coefficient of variation of each pixel was calculated among the different image dates in order to assess the interdate variability of the textures measures (Fig. 3). With three study sites, six bands, four first-order measures with three window sizes, and seven second-order measures with two window sizes, this processing yielded 216 single-band coefficient of variation images for first-order texture measures and

TABLE II
IMAGE TEXTURE MEASURE FORMULAE

| **Type of Measure** | **Texture Measure** | **Formula [11,22]** |
|---|---|---|
| **1st Order** | **Mean** | $\dfrac{\sum_{k=1}^{N} x_k}{N}$<br>Where N = the number of pixels in the window, and, $x_k$ = the gray tone value of pixel k. |
| | **Variance** | $\dfrac{1}{N-1}\sum_{k=1}^{N}(x_k-\bar{x})^2$ |
| | **Entropy** | $-\sum_{g=1}^{G} P(g)\log[P(g)]$<br>Where G = the number of gray tone levels, and P(g) is the probability of occurrence of gray level g in the window. |
| | **Skewness** | $\dfrac{\frac{1}{N}\sum_{k=1}^{N}(x_k-\bar{x})^3}{\left(\frac{1}{N}\sum_{k=1}^{N}(x_k-\bar{x})^2\right)^{3/2}}$ |
| **2nd Order** | **Angular Second Moment** | $\sum_i\sum_j\{p(i,j)\}^2$<br>Where p(i,j) is the (i,j)th entry in the normalized GLCM |
| | **Correlation** | $\dfrac{\sum_i\sum_j (ij)p(i,j)-\mu_x\mu_y}{\sigma_x\sigma_y}$<br>Where $\mu_x$, $\mu_y$, $\sigma_x$, and $\sigma_y$ are the means and standard deviations of $p_x$ and $p_y$, where $p_x$ and $p_y$ are the marginal probabilities of x and y in the normalized GLCM |
| | **Contrast** | $\sum_{n=0}^{N-1} n^2\left\{\sum_{i=1}^{N}\sum_{j=1}^{N} p(i,j)\right\}$<br>**where n =** $\lvert i-j\rvert$ |
| | **Homogeneity (IDM)** | $\sum_i\sum_j \dfrac{1}{1+(i-j)^2}p(i,j)$ |
| | **Dissimilarity** | $\sum_{n=0}^{N-1} n\left\{\sum_{i=1}^{N}\sum_{j=1}^{N} p(i,j)\right\}$ |
| | **Entropy** | $-\sum_i\sum_j p(i,j)\log(p(i,j))$ |
| | **Variance** | $\sum_i\sum_j (i-\mu)^2 p(i,j)$ |

252 images for second-order texture measures (Fig. 4). To facilitate comparison between texture measures, cloud-contaminated areas were masked, and the image-wide mean was calculated for each of the single-band coefficient of variation images.

## III. RESULTS

All study sites showed substantial interseasonal variation in both first- and second-order texture measures. The overall mean coefficients of variation of the calculated texture measures were 0.52, 0.66, and 1.06 for the New Mexico, Ontario, and Virginia

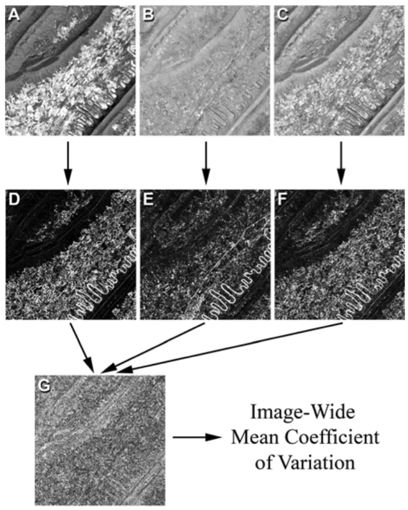


Fig. 3. Processing flow example for a subset of Virginia study site. Original images, TM Band 4, 03/31/2000 (a), 05/24/2002 (b), 10/15/1999 (c). First-order variance TM band 4 $3 \times 3$ window size 03/31/2000 (d), 05/24/2002 (e), 10/15/1999 (f). Pixel-wise coefficient of variation across dates (g).

study sites, respectively. These levels are higher than we expected, and it can be seen that the level of variation was substantially higher in the Virginia study site. As a test sample, a small area of evergreen forest was selected from the Ontario study site, and $11 \times 11$ second-order texture measures of this area were plotted for each of the four image dates (Fig. 5). The two images from very early in the growing season (04/29/00 and 05/21/2002) showed very similar texture measures. However, during the peak of the growing season (07/05/2001) most texture measures changed substantially in value. Entropy, contrast, variance, and dissimilarity show a marked increase in value, while correlation and homogeneity show a decrease. Late in the growing season (09/12/2000) texture measures returned to values similar to the two early images.

The ranking of seasonal variation in first-order texture measures was consistent between the Ontario and New Mexico sites with entropy and mean as the least variable measures, followed by variance, then skew (Fig. 6). While the relative ordering of variability in texture measures of the Virginia site was similar, entropy, mean, and variance had noticeably higher seasonal variability. The variability of skew was similar in all three sites and substantially higher than the three other measures. Overall variation was high for variance and skew, with a mean coefficient of variation of approximately 0.7 and 1.75, respectively.

Seasonal variability of second-order texture measures was fairly complex (Fig. 7). Variability of contrast, dissimilarity, entropy, homogeneity, and variance were very similar between the New Mexico and Ontario sites, with the New Mexico site being slightly less variable in each case. Differences between Ontario and New Mexico were much larger for angular second moment and correlation. Homogeneity and entropy were the most robust measures in these two sites, followed by dissimilarity, contrast, and variance. However, the variation of texture measures of the Virginia site was substantially higher, with most coefficients of variation near 1.0. It is difficult to ascertain the relative robustness of angular second moment and correlation given that the level of variation was inconsistent among the three study sites.

There were noticeable differences in robustness of texture measures among biomes. The Virginia site had the highest level of variation in 9 of the 11 texture measures, for an overall average coefficient of variation of 1.06. For most of the texture measures, the level of variation was similar between the New Mexico and Ontario sites, with New Mexico yielding a slightly lower overall mean coefficient of variation of 0.52 compared to 0.66 for the Ontario site.

With regard to window size, there appeared to be a slight trend of decreasing interseasonal variability with increasing window size when comparing coefficients of variation averaged across all bands and texture measures (Fig. 8).

It was expected that texture measures of different Landsat spectral bands would behave differently with regard to robustness to seasonal change. Band 4 (near infra-red) was of particular interest as this band is especially sensitive to vegetative vigor, which varies substantially over the growing season. Measures calculated from band 4 did not show substantially higher interseasonal variation than those of other bands. The mean per-band level of variability averaged across all texture measures was relatively constant for first order measures (Fig. 9), with the exception of band 3 in the New Mexico and Ontario site and band 4 in the Ontario site.

The mean per-band variability averaged across second-order texture measures showed a stronger pattern (Fig. 10). Once again, the Virginia site consistently had the highest variation. Ontario and New Mexico showed higher variability between bands and followed a similar pattern with the coefficient of variation increasing to a peak around band 3 then decreasing.

Although some texture measures appeared to vary similarly across an individual study site, with other textures, patterns did emerge. For example, in the Virginia study site, homogeneity showed noticeable differences in coefficient of variation between the agricultural areas in the valleys, and the mountainous forested areas [Fig. 4(d)–(f)]. The coefficient of variation for band 4 was strikingly higher in the agricultural areas. Homogeneity heavily weights the main diagonal of the GLCM, so areas composed of many adjacent pixels with highly similar DNs yielded a high value. In agricultural areas, homogeneity was very high within-field, and low between fields, especially in this study site where some images contained vegetatively active fields (high NIR/red ratio) adjacent to fields with low activity (nearly even NIR/red ratio). In contrast, while the forested mountainous areas varied in band 4 values over the growing season, each forested area varied relatively consistently, resulting in a smaller coefficient of variation for homogeneity. This highlights the importance of considering land cover and texture characteristics of the setting of interest when considering the effects of vegetation phenology on texture measures.

## IV. Discussion

The most significant finding of our study was that all texture measures varied substantially with phenology. This variation can significantly impact analyses utilizing texture measures

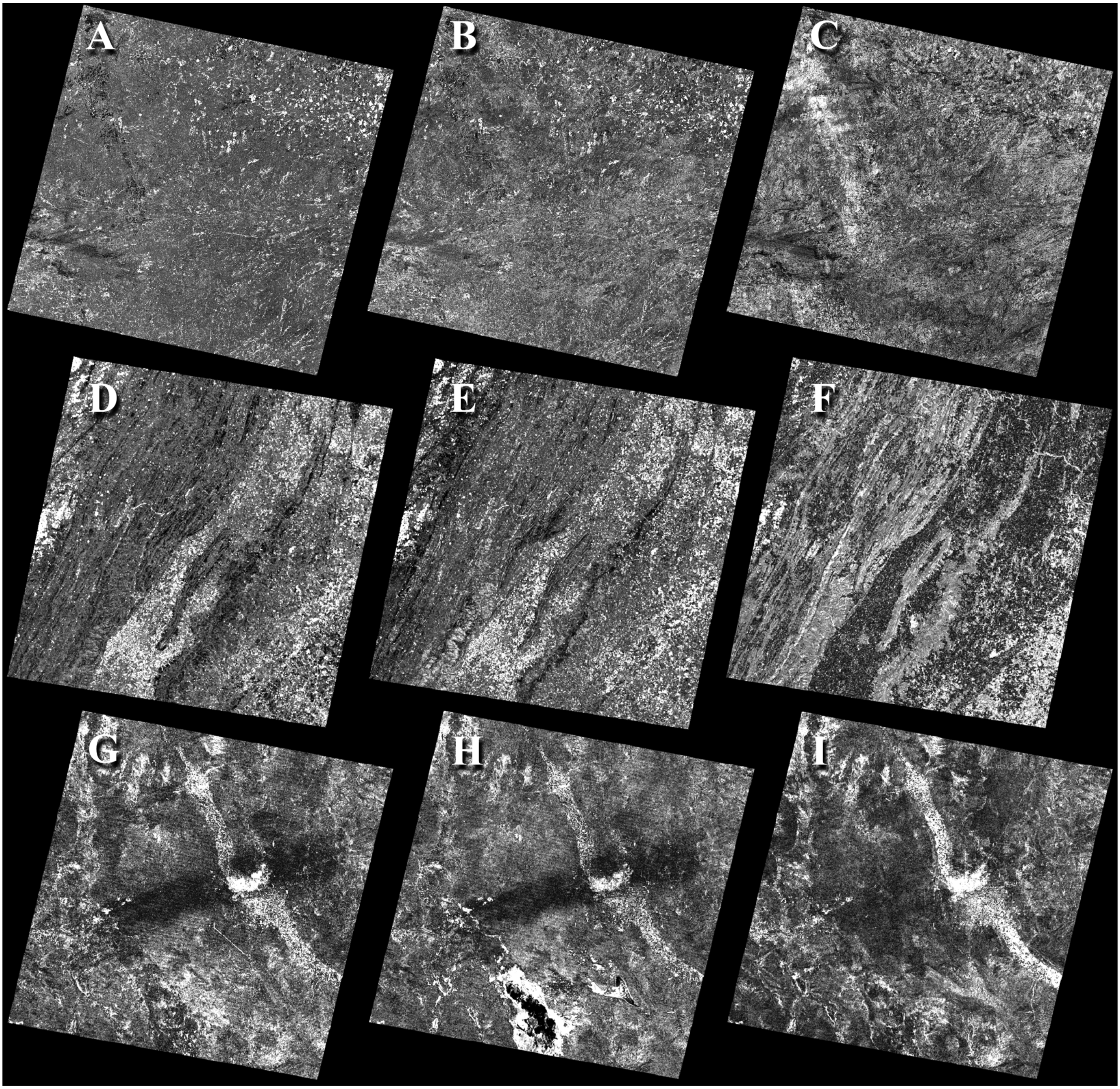


Fig. 4. Sample of the 468 single-band interseasonal coefficient of variation images. (a)–(c) Ontario study site, first-order variance, 7 × 7 window size, bands 2, 3, and 4, respectively. (d)–(f) Virginia study site, second-order contrast, 15 × 15 window size, bands 2, 3, and 4, respectively. (g)–(i) New Mexico study site, second-order homogeneity, 15 × 15 window size, bands 2, 3, and 4, respectively.

and should be of special concern in studies using multitemporal imagery or a very large spatial extent requiring many images. Even in single-date, single-image analyses, care should be taken in the choice of image date, as the textural measures of specific features will vary based on the phenological stage of the image.

While overall variation was high, some patterns did emerge. Among the three study sites, first-order measures were consistently ranked in their robustness to phenological variation, with mean and entropy being the most robust, followed by variance then skew. In contrast, no clear pattern of robustness emerged in second-order measures, as the Virginia site did not follow the patterns observed at the other sites. Because of this, it is inconclusive if there is a consistent ordering of robustness of second-order texture measures, although homogeneity, entropy, and dissimilarity appeared to be the most robust.

One of our more striking results was that while the boreal forest of Ontario was a substantially different ecosystem than the desert scrub of southern New Mexico, both sites behaved quite similarly with respect to interseasonal variability in both first- and second-order texture measures. We expected the Virginia site to behave similar to the Ontario site, since both are heavily forested, but found substantial differences.

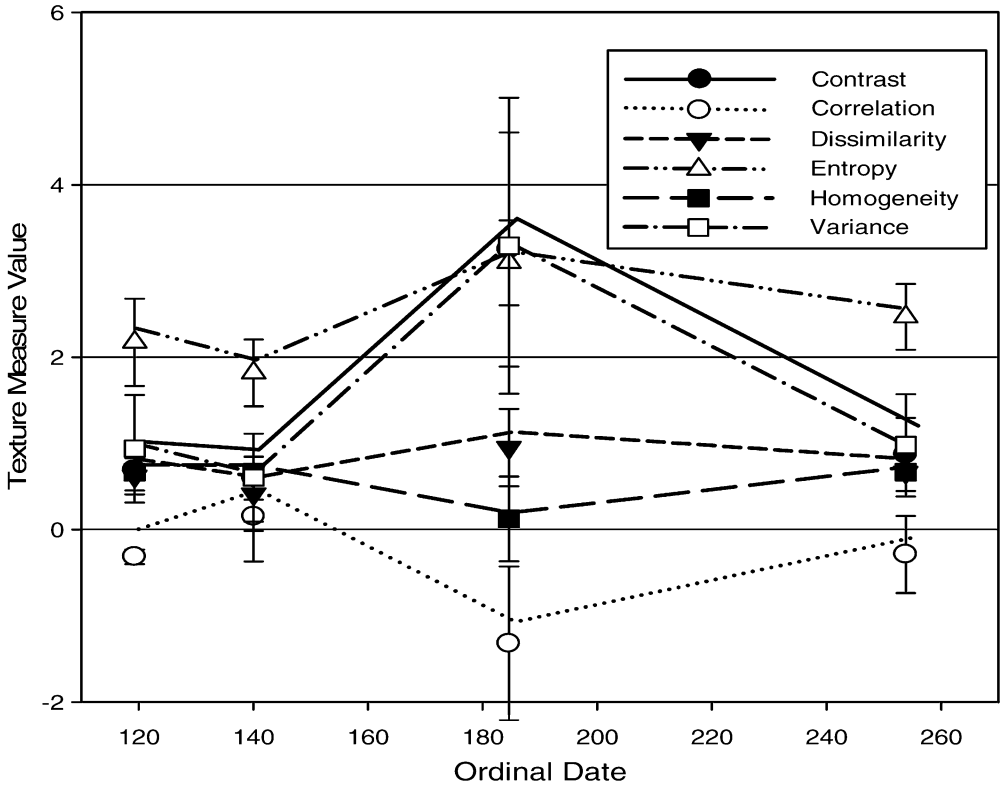


Fig. 5. Mean values of 11 × 11 second-order texture measures of TM band 4 across the growing season for a small area of primarily coniferous forest in the Ontario site. Little variation occurred between the first two dates, which both occurred very early in the growing season. The peak of the growing season showed a substantial difference in texture measures. In the final date, which is in the late growing season, texture measures reverted close to early growing season levels. Error bars indicate plus and minus one standard deviation.

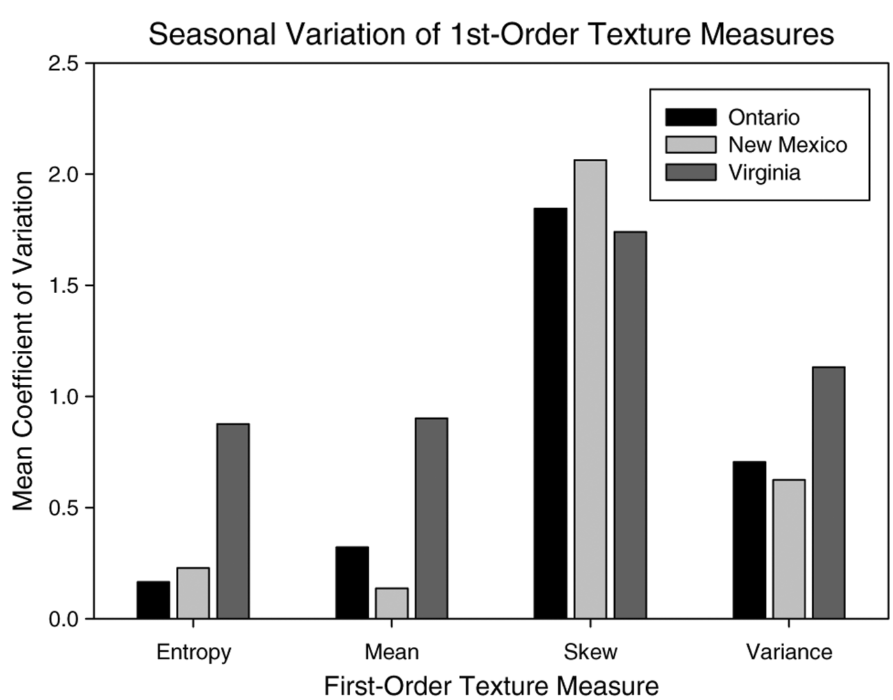


Fig. 6. Mean image-wide coefficient of variation of first-order texture measures averaged across bands and three window sizes, for the three study sites. Entropy and mean had the lowest coefficient of variation. The Ontario and New Mexico study sites behaved similarly. Variation was generally higher in the Virginia site with a less distinct ranking of texture measure robustness.

One possible explanation is the relatively large areas of agriculture in the Virginia site. The Ontario site had no agriculture and the New Mexico site had a limited amount. Agricultural fields can show substantial spectral variability across the

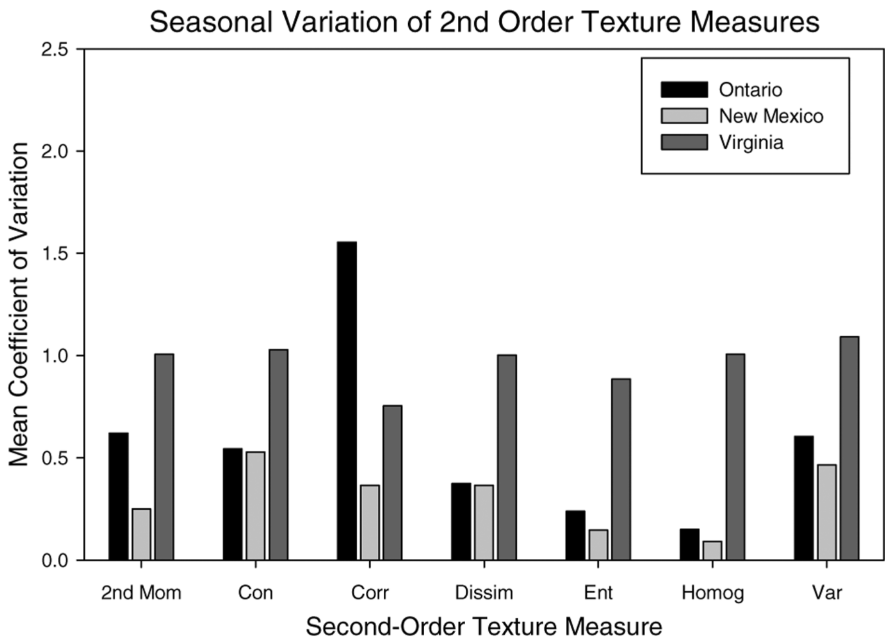


Fig. 7. Mean image-wide coefficient of variation averaged across bands and three window sizes for each study site. Homogeneity and entropy were the most robust second-order measures. The Ontario and New Mexico sites behaved similarly. The Virginia site had higher variation and less distinction in robustness between different texture measures.

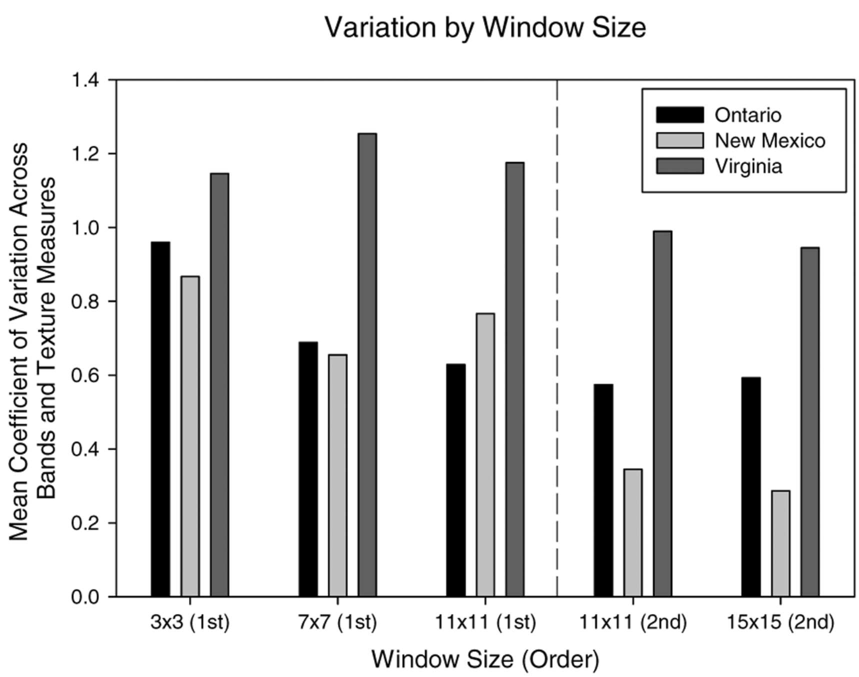


Fig. 8. Mean coefficient of variation in texture measures summarized for first- and second-order measures for each window size. The mean coefficient of variation shows a slight decreasing trend as window size increases.

growing season, potentially greatly increasing interseasonal variability.

To further investigate this, we manually selected several areas of agriculture and forest in the Virginia study site and compared their interseasonal variability. Contrary to our expectation, the overall mean level of variability was nearly identical between the two classes, with a mean coefficient of variation of 0.98 for agriculture, and 1.09 for forest. Therefore, the higher level of agriculture in the Virginia study site did not explain the site's higher variability.

As we expected, interseasonal variability in texture measures was relatively unaffected by the window size chosen for the texture calculations. This allows the flexibility to choose a window size based on a spatial scale(s) that is appropriate for a specific research question [3], [31] as long as the window is large enough to avoid sparsely populated GLCMs [24].

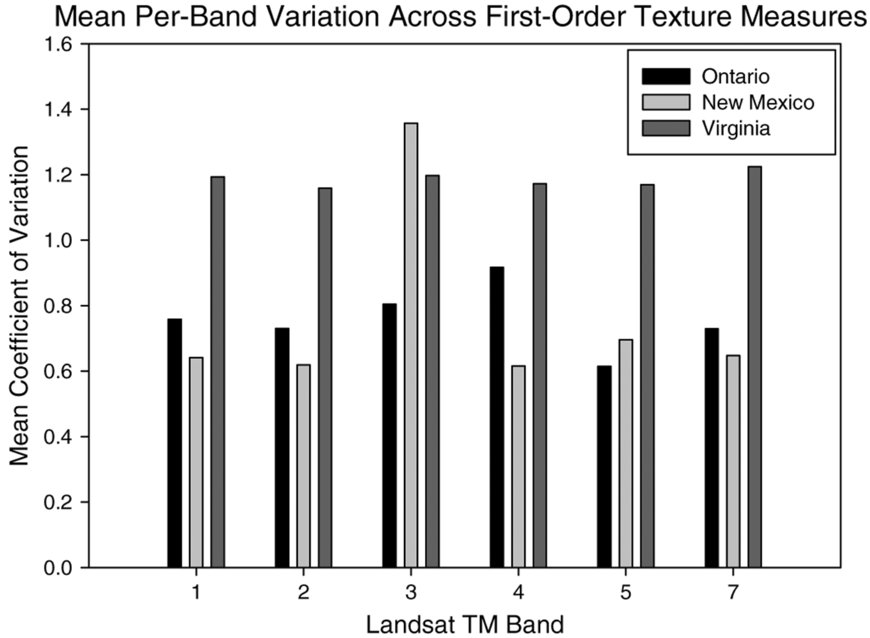


Fig. 9. Mean variation in first order measures by band. Most bands behaved similarly with a slightly higher level of variation in bands 3 and 4.

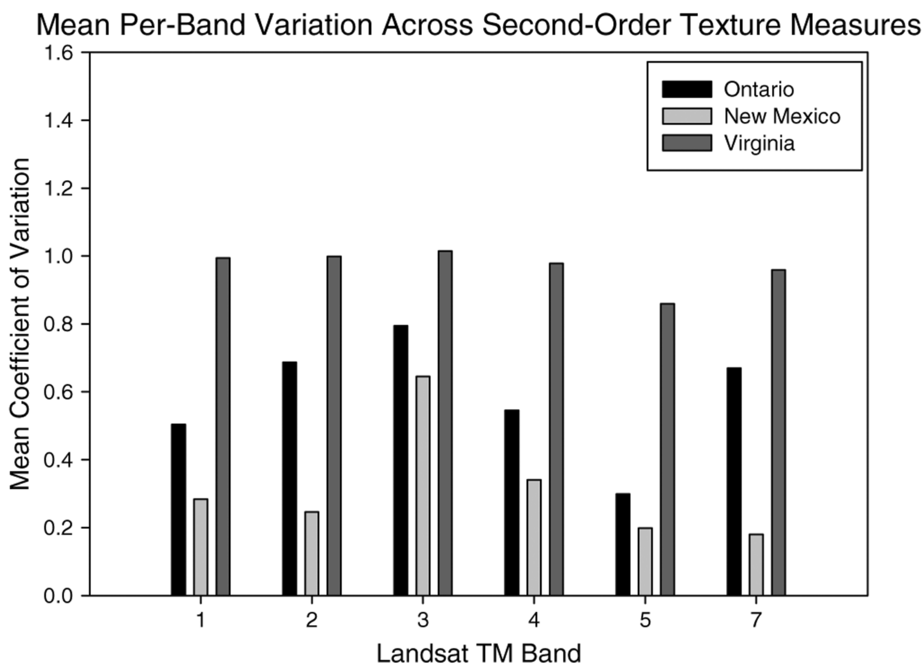


Fig. 10. Mean variation in second-order measures by band. Variation was less consistent overall with an apparent peak at band 3.

In contrast to our predictions, robustness to interseasonal variability was relatively consistent across spectral bands, especially for first-order texture measures. Our findings imply that there are not specific spectral bands that are universally more sensitive to phenological variation than others.

We believe most of the observed variability in the texture measures can be attributed to changes in phenology, but other factors may have contributed to the variability. As with all studies using imagery from different points of the year, sun angle varies between images, yielding different illumination. In areas of more complex vertical structure, such as forests, this lighting effect will be more pronounced, due to sunlit portions of crowns being brighter, and due to shadows cast by taller trees. These changes in highlight and shadow will yield changes in texture measures. It is also possible that atmospheric conditions varied among (and within) the images, and we did not apply atmospheric correction in this study. Atmospheric contamination can reduce the contrast of an image, which would reduce the values of texture measures responding to heterogeneity (e.g., variance), and increase the value of texture measures that respond to homogeneity (e.g., angular second moment). As with all multitemporal analyses, precise co-registration of imagery is very important. Misregistration between image dates would artificially inflate variability because the texture values would be calculated from a slightly different area in each image. Lastly, because the imagery used in our study was not all acquired during the same year, in addition to the large seasonal differences in the images, there were likely some interannual differences contributing to variability.

Remote sensing has been used to explicitly monitor vegetation phenology [32]–[34]. Much of the effort has focused on using time series to monitor vegetation phenology over very large spatial extents, often continental scale, from coarse spatial resolution imagery. The goal of these analyses is often to track specific points in vegetation phenology such as greenup or senescence over many years to monitor temporal shifts in phenology. Thus far, there have been relatively few mentions of the effect of phenology on texture measures. Many studies using measures of texture have relied on single-date imagery [3], [4], [7], [9], [10], [12], [15], [16], [18], [35], [36], and little mention was made regarding the choice of date in relation to texture measures. It is important to consider how texture measures may vary over the growing season in relation to the feature of interest. Even within the growing season, there may be specific windows of time during which certain texture measures will be most powerful in discerning the feature of interest.

It is critical that future studies consider the effects of phenology on texture measures. Some existing multitemporal studies using texture measures [17], [24], [25] have utilized anniversary date imagery, with some making explicit references to concern over phenological changes. However, the specific effect of phenology on texture measures was not explored.

Thus far, few studies have carried out texture analysis over very large spatial extents. In a study modeling bird species occurrence [6], textures measures were calculated from a 2001 Landsat TM mosaic of the state of Maine. It was unclear if the mosaic used same date imagery. Such large spatial extent studies are likely to increase in number as technical capabilities allow. In these cases the effects of phenology must be carefully considered, as cloud cover and other natural variability makes it difficult to create large image mosaics with all images on the same date or even within the same month.

Several actions can be taken to minimize the effect of phenological variation on texture measures. Foremost, whenever possible, imagery should be selected for the same date or phenological stage. The texture measures chosen should be based on the specific application, but if possible, measures that are more robust to phenological variation should be selected, such as first-order mean or entropy, or second-order homogeneity, entropy, or dissimilarity. Special attention should be paid to land cover types, such as agriculture, that show high interseasonal or interannual variability. Just as it is advisable to explore different texture measures and parameter settings for a specific application, the effects of seasonality should be explored in small test areas when possible.

The upside to phenological variation in image texture is that these changes may contain important information. As Fig. 5 shows, a land cover class (in this case evergreen forest) can show a strong change in texture measures with change in phenology. With higher temporal resolution, the behavior of each texture measure could be further teased out to determine a more precise pattern. When these patterns are known for other land cover types or features of interest, the variability in texture measure can be exploited by choosing imagery at a specific phenological stage or stages to yield the best results.

The phenological variation of texture measures can also be exploited in image classification. Multitemporal classification of spectral data has been shown to improve classification accuracy over single-date classifications [37]. For example, some broadleaf tree species are spectrally similar during the growing season, but green-up and senesce at different time points; thus, a multitemporal classification that includes imagery across these points can yield higher accuracy than a single date classification [38]. A similar approach utilizing texture measures instead of spectral values seems promising and warrants further exploration.

Before this can be done, more understanding is needed on the trends of specific texture measures in different biomes over the growing season, and which parts of the growing season yield the best measures to characterize a specific process.

## Acknowledgment

The authors would like to thank P. Townsend who graciously supplied the Virginia and Ontario images. They would also like to thank C. Kingdon and M. Dubinin for guidance in regard to the image texture processing, the associate editor, for thorough and constructive comments, and the two anonymous reviewers, as their suggestions greatly improved this manuscript.

## References

[1] R. M. Haralick, "Statistical and structural approaches to texture," *Proc. IEEE*, vol. 67, pp. 786–804, 1979.

[2] A. Baraldi and F. Parmiggiani, "An investigation of the textural characteristics associated with gray-level cooccurrence matrix statistical parameters," *IEEE Trans. Geosci. Remote Sens.*, vol. 33, no. 3, pp. 293–304, Mar. 1995.

[3] C. A. Coburn and A. C. B. Roberts, "A multiscale texture analysis procedure for improved forest stand classification," *Int. J. Remote Sens.*, vol. 25, pp. 4287–4308, Oct. 2004.

[4] S. E. Franklin, A. J. Maudie, and M. B. Lavigne, "Using spatial co-occurrence texture to increase forest structure and species composition classification accuracy," *Photogramm. Eng. Remote Sens.*, vol. 67, pp. 849–855, July 2001.

[5] S. E. Franklin, R. J. Hall, L. M. Moskal, A. J. Maudie, and M. B. Lavigne, "Incorporating texture into classification of forest species composition from airborne multispectral images," *Int. J. Remote Sens.*, vol. 21, pp. 61–79, Jan. 10, 2000.

[6] J. A. Hepinstall and S. A. Sader, "Using Bayesian statistics, thematic mapper satellite imagery, and breeding bird survey data to model bird species probability of occurrence in Maine," *Photogramm. Eng. Remote Sens.*, vol. 63, pp. 1231–1237, Oct. 1997.

[7] E. M. Tuttle, R. R. Jensen, V. A. Formica, and R. A. Gonser, "Using remote sensing image texture to study habitat use patterns: A case study using the polymorphic white-throated sparrow (Zonotrichia albicollis)," *Global Ecol. Biogeogr.*, vol. 15, pp. 349–357, Jul. 2006.

[8] L. D. Estes, G. S. Okin, A. G. Mwangi, and H. H. Shugart, "Habitat selection by a rare forest antelope: A multi-scale approach combining field data and imagery from three sensors," *Remote Sens. Environ.*, vol. 112, pp. 2033–2050, May 15, 2008.

[9] A. L. Wunderle, S. E. Franklin, and X. G. Guo, "Regenerating boreal forest structure estimation using SPOT-5 pan-sharpened imagery," *Int. J. Remote Sens.*, vol. 28, pp. 4351–4364, 2007.

[10] F. Kayitakire, C. Hamel, and P. Defourny, "Retrieving forest structure variables based on image texture analysis and IKONOS-2 imagery," *Remote Sens. Environ.*, vol. 102, pp. 390–401, 2006, 6/15.

[11] R. M. Haralick, K. Shanmuga, and I. Dinstein, "Textural features for image classification," *IEEE Trans. Syst., Man, Cybern.*, vol. SMC-3, pp. 610–621, 1973.

[12] S. Tuominen and A. Pekkarinen, "Performance of different spectral and textural aerial photograph features in multi-source forest inventory," *Remote Sens. Environ.*, vol. 94, pp. 256–268, Jan. 30, 2005.

[13] H. B. Musick and H. D. Grover, "Image textural measures as indices of landscape pattern," in *Quantitative Methods in Landscape Ecology*, M. G. Turner and K. J. Gaston, Eds. New York: Springer-Verlag, 1991, pp. 77–103.

[14] B. Tso and P. Mather, *Classification Methods for Remotely Sensed Data*. London, U.K.: Taylor & Francis, 2001, pp. 212–216.

[15] K. Johansen, N. C. Coops, S. E. Gergel, and Y. Stange, "Application of high spatial resolution satellite imagery for riparian and forest ecosystem classification," *Remote Sens. Environ.*, vol. 110, pp. 29–44, Sept. 14, 2007.

[16] S. E. Franklin, M. A. Wulder, and G. R. Gerylo, "Texture analysis of IKONOS panchromatic data for Douglas-Fir forest age class separability in British Columbia," *Int. J. Remote Sens.*, vol. 22, pp. 2627–2632, Sep. 10, 2001.

[17] A. T. Hudak and C. A. Wessman, "Textural analysis of historical aerial photography to characterize woody plant encroachment in South African savanna," *Remote Sens. Environ.*, vol. 66, pp. 317–330, Dec. 1998.

[18] M. A. Wulder, E. F. LeDrew, S. E. Franklin, and M. B. Lavigne, "Aerial image texture information in the estimation of northern deciduous and mixed wood forest leaf area index (LAI)," *Remote Sens. Environ.*, vol. 64, pp. 64–76, Apr. 1998.

[19] M. L. Cody, "Habitat selection in birds—The roles of vegetation structure, competitors, and productivity," *Bioscience*, vol. 31, pp. 107–113, 1981.

[20] R. H. MacArthur and J. W. MacArthur, "On bird species diversity," *Ecology*, vol. 42, pp. 594–598, Jul. 1961.

[21] L. M. Bellis, A. M. Pidgeon, V. C. Radeloff, V. St.-Louis, J. L. Navarro, and M. B. Martella, "Modeling habitat suitability for greater rheas based on satellite image texture," *Ecol. Appl.*, to be published.

[22] V. St.-Louis, A. M. Pidgeon, V. C. Radeloff, T. J. Hawbaker, and M. K. Clayton, "High-resolution image texture as a predictor of bird species richness," *Remote Sens. Environ.*, vol. 105, pp. 299–312, Dec. 30, 2006.

[23] V. St.-Louis, A. M. Pidgeon, M. K. Clayton, B. A. Locke, D. Bash, and V. C. Radeloff, "Satellite image texture and a vegetation index predict avian biodiversity in the Chihuahuan desert of New Mexico," *Ecography*, to be published.

[24] C. Vega-Garcia and E. Chuvieco, "Applying local measures of spatial heterogeneity to Landsat-TM images for predicting wildfire occurrence in Mediterranean landscapes," *Landscape Ecol.*, vol. 21, pp. 595–605, May 2006.

[25] P. Peroni, F. Ferri, and G. C. Avena, "Temporal and spatial changes in a mountainous area of central Italy," *J. Veg. Sci.*, vol. 11, pp. 505–514, Aug. 2000.

[26] C. J. Tucker, "Red and photographic infrared linear combinations for monitoring vegetation," *Remote Sens. Environ.*, vol. 8, pp. 127–150, 1979.

[27] R. G. Bailey, Description of the Ecoregions of the United States, U.S. Dept. Agriculture, 1995.

[28] E. B. Wiken, *Terrestrial Ecozones of Canada. Ecological Land Classification Series No. 19*. Hull, QC, Canada: Environment Canada, 1986.

[29] ERDAS Imagine 2005, Leica Geosystems, v. 9.0. [CD-ROM].

[30] ENVI 2005, Research Systems Inc., v. 4.2. [CD-ROM].

[31] S. E. Franklin, M. A. Wulder, and M. B. Lavigne, "Automated derivation of geographic window sizes for use in remote sensing digital image texture analysis," *Comput. Geosci.*, vol. 22, pp. 665–673, Jul. 1996.

[32] B. C. Reed, J. F. Brown, D. VanderZee, T. R. Loveland, J. W. Merchant, and D. O. Ohlen, "Measuring phenological variability from satellite imagery," *J. Veg. Sci.*, vol. 5, pp. 703–714, Nov. 1994.

[33] X. Zhang, M. A. Friedl, C. B. Schaaf, A. H. Strahler, J. C. F. Hodges, F. Gao, B. C. Reed, and A. Huete, "Monitoring vegetation phenology using MODIS," *Remote Sens. Environ.*, vol. 84, pp. 471–475, 2003, 3.

[34] R. Stockli and P. L. Vidale, "European plant phenology and climate as seen in a 20-year AVHRR land-surface parameter dataset," *Int. J. Remote Sens.*, vol. 25, pp. 3303–3330, Sept. 2004.

[35] P. C. Smits and A. Annoni, "Updating land-cover maps by using texture information from very high-resolution space-borne imagery," *IEEE Trans. Geosci. Remote Sens.*, vol. 37, no. 5, pp. 1244–1254, May 1999.

[36] D. R. Peddle and S. E. Franklin, "Image texture processing and data integration for surface pattern-discrimination," *Photogramm. Eng. Remote Sen.*, vol. 57, pp. 413–420, Apr. 1991.

[37] C. Homer, C. Huang, L. Yang, B. Wylie, and M. Coan, "Development of a 2001 national land-cover database for the United States," *Photogramm. Eng. Remote Sen.*, vol. 70, pp. 829–840, Jul. 2004.

[38] P. T. Wolter, D. J. Mladenoff, G. E. Host, and T. R. Crow, "Improved foresty classification in the northern lake states using mult-temporal Landsat imagery," *Photogramm. Eng. Remote Sens.*, vol. 61, pp. 1129–1143, Sep. 1995.


**Patrick D. Culbert** received the B.S. degree in forest science and computer science from the University of Wisconsin-Madison in 2004, where he is currently pursuing the M.S. degree in biometry and the Ph.D. degree in forestry.

From 2004 to 2006, he was a Remote Sensing Analyst at Ocean Imaging, Solana Beach, CA. There, he developed and implemented image processing algorithms related to the identification and thickness estimation of marine oil spills from multispectral aerial imagery.

Mr. Culbert is a member of the Society of American Foresters and the American Society for Photogrammetry and Remote Sensing.

**Anna M. Pidgeon** received the B.S. degree in wildlife management and life science education from the University of Minnesota, the M.S. degree in biology from Central Washington University in 1995, and the Ph.D. degree in wildlife ecology from the University of Wisconsin-Madison in 2000.

She was a Scientist in the Department of Forest and Wildlife Ecology, University of Wisconsin-Madison, conducting research in avian ecology from 2000 to 2007. In 2008, she became an Assistant Professor in the same department, and teaches vertebrate ecology in addition to conducting research.

Prof. Pidgeon is a member of the American Ornithologists Union, the Cooper Society, the Inland Bird Banding Association, The Wildlife Society, and the Society for Conservation Biology.

**Véronique St.-Louis,** received the B.S. degree in biology-wildlife management from the Université du Québec à Rimouski in 1998, the M.S. degree in biological sciences from the Université de Montréal in 2000, and the Ph.D. degree in forest ecology and the M.S. degree in biometry from the University of Wisconsin-Madison in 2009.

After receiving the M.S. degree in 2000, she spent two years at the Canadian Wildlife Service of Environment Canada managing and analyzing data for the Ontario Forest Bird Monitoring program.

Dr. St.-Louis is a member of the Canadian Society for Ecology and Evolution, the Ecological Society of America, and the International Association of Landscape Ecology.

**Dallas Bash,** photograph and biography not available at the time of publication.

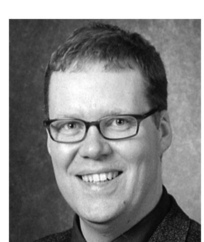

**Volker C. Radeloff** received the diploma in geography from the University of Trier, Germany, in 1994, the M.S. degree in GIS from Edinburgh University, U.K., 1995, and the Ph.D. degree in forestry from the University of Wisconsin-Madison in 1998.

He has been a faculty member in the Department of Forest and Wildlife Ecology, University of Wisconsin-Madison, since 2000, where he teaches classes in forest biometry and conducts research at the interface of remote sensing, GIS, and conservation biology.

Prof. Radeloff is a member of the American Society for Photogrammetry and Remote Sensing, the Ecological Society of America, and the Society for Conservation Biology.